Jurnal Kejuruteraan 38(5) 2026: 2203-2220
https://doi.org/10.17576/jkukm-2026-38(5)-10

Lignin Extraction from Coconut Pith by Alkaline and Organosolv Treatment: Characterization and Optimization of Lignin Yield and Purity

Mai Syadiah Khidzir[a], Siti Musliha Mat Ghani[a], Abdul Rahman Abdul Rahim[a] & Khairirahanna Johari[a,b*]

[a]*Department of Chemical Engineering, Universiti Teknologi PETRONAS (UTP), 32610 Seri Iskandar, Perak Darul Ridzuan, Malaysia*

[b]*Centre for Carbon Capture, Utilization and Storage (CCUS), Universiti Teknologi PETRONAS (UTP), 32610 Seri Iskandar, Perak Darul Ridzuan, Malaysia*

[*]*Corresponding author: khairiraihana.j@utp.edu.my*

Received 30 August 2025, Received in revised form 2 March 2026
Accepted 2 April 2026, Available online 30 August 2026

ABSTRACT

Effective coconut pith lignin (CPL) extraction remained an obstacle since lignin must be removed without causing significant destruction of cellulose fibers. This work seeks to solve these challenges by improving the extraction procedure for CPL to generate a material appropriate for industrial uses, such as anti-corrosion coatings, that take advantage of lignin's distinct features. A comprehensive technique based on response surface methodology (RSM) and central composite design (CCD) was used to optimize three critical process parameters: temperature, solvent concentration and time of alkaline treatment (AT) and organosolv treatment (OT) concentration for extracting the lignin. The screening findings showed that the AT produced the highest yield of lignin and purity compared to the OT. This will provide 72.29% CPL-AT and 86.00% purity through RSM analysis. (TGA) and (FTIR) were used to assess the physical qualities of lignin. Fourier transform infrared (FTIR) analysis demonstrated that CPL-AT and CPL-OT possess similar spectrums, though the CPL-OT showed more prominent peaks of aromatic rings and phenolic hydroxyl groups. Thermogravimetric analysis (TGA) studies demonstrated that CPL-AT has higher heat stability owing to its higher molecular weight and solubility properties which makes it has potential and economically viable material for industrial applications such as bio-composite materials.

Keywords: Coconut pith; extraction; lignin; purity; yield

INTRODUCTION

Coconut pith (CP), or *Cocos nucifera L*., is a byproduct of the coconut crop that has attracted much attention due to its feasible usage in biorefinery processing. Every year, 24 and 31 million tons of coconut waste are produced globally, most of which are burned (Sand & Tuteja 2022). Although CP is a waste product, its high lignin content (up to 50% by weight) makes it a potentially valuable material in many chemical businesses. Lignin is frequently regarded as a low-value by-product in biorefineries, and it is typically combusted to produce process heat. However, this approach underutilizes lignin's potential as a valuable precursor for high-value products. Instead of combustion, CP lignin (CPL) can be transformed into specialty chemicals, biofuels, and advanced materials, enhancing economic value and sustainability while supporting a zero-waste biorefinery model. The global lignin market is expected to reach USD 913.1 million by 2025, growing at a 2.2% Compound Annual Growth Rate (CAGR) due to increased use in biofuels, carbon fibers for the automotive and aerospace industries, and energy storage technologies such as supercapacitors and batteries (Bajwa et al. 2019; Espinoza-Acosta et al. 2018; Souto et al. 2018). This highlights CPL's status as a renewable alternative to petrochemicals due to its transition to sustainable materials.

CPL has unique structural and functional advantages over lignin from other biomass sources, such as wood (20-30% lignin) or agricultural waste like straw and corn stover (Anuchi, Sedransk Campbell et al. 2022). The CPL acts as a natural adhesive, shaping the coconut husk. High lignin

and hydrophobic waxes make the fibers strong and water-resistant. That helps the material maintain longer and resist microorganisms. Since CP is porous, air can move through it, but water cannot, making it more resistant to breakdown. This causes it to be preserved in the long term and can be suitable to apply in several needs. CPL's complicated phenylpropane structure with multiple functional groups makes it distinctive. It's ideal for corrosion-resistant coatings because of its aromatic ring structure. It prevents corrosion on metal surfaces using an antioxidant barrier so that it can last longer in severe environments and can act as better UV blocking. The uniqueness of CPL compared to other biomass lignin also shows that it is more stable due to its high carbon-to-oxygen ratio and moderate breakdown rate.

To extract CPL, the chemical interactions between lignin, hemicellulose, and acetyl groups must first be disrupted by the treatment. One of the favored treatments is alkaline treatment with sodium hydroxide (NaOH), often favored owing to its overall efficacy in removing lignin (Singh et al. 2015). This preference is not only inexpensive and readily available on a large scale but also highly effective at disrupting the complex lignin-carbohydrate matrix in many biomasses as it selectively targets lignin over other components like cellulose and hemicellulose because NaOH tends to degrade lignin less, allowing the resulting in lignin maintaining a higher molecular weight and potentially better properties for its subsequent uses. Bali et al. (2015) found that NaOH treatment improves the breakdown of materials with low lignin contents. Furthermore, its great solubility in water makes it simple to use since it stays constant throughout the reaction mixture. This selectivity is practical for options that aim to produce high-purity lignin while maintaining the integrity of other key elements.

Additionally, the organosolv treatment is an eco-friendly method that utilizes less harmful chemicals that may be reused. Using organic acids, methanol, acetone, or ethanol with one another or with water is feasible. Most solvents need high temperatures and pressures to penetrate the CP structure and break lignin-carbohydrate linkages (Yousuf et al. 2020). The extracted lignin is relatively pure and may be utilized to make high-value goods like bio-based polymers, resins, and fuel. The liquid fraction is treated with an anti-solvent to initiate precipitation and extract the lignin. The solvent is often recovered and returned to the system by distillation, making the process more affordable and ecologically beneficial (Yadav et al. 2021).

A critical evaluation of various parameters, such as the concentrations, temperature, and duration, can be undertaken to improve the process by optimizing the lignin yield through all of these treatments. For NaOH treatment, increasing NaOH concentrations increases lignin solubilizing efficiency. There is still an optimal range beyond which the degradation of lignin and hemicellulose may affect the benefits (Bali et al. 2015). Kaur et al. (2015) conducted lignin extraction using different concentrations of NaOH solutions and found that the maximum lignin yield was 10 % NaOH. However, Wunna et al. (2021) discovered that the highest delignification in sugar bagasse was achieved with a 2 wt.% concentration of NaOH and a 30-minute residence duration in an autoclave. This may be due to the biomasses with more accessible lignin or less complex structures responding better to the treatment. Besides, decreased particle sizes of the biomass enhance the surface area for solvent penetration, improving the interaction and yield of lignin extraction (Kumar et al. 2017). The preliminary treatment methods, such as milling or microwave-assisted treatment, can improve biomass's surface area and permeability This will make the solvent easy to solubilize and disrupt lignin's wall during the extraction process (Anuchi, Hallett et al. 2022). Physical treatment like proper mixing and agitation also improves lignin's mass transfer and solubilization.

Lin et al. (2020) discovered that elevated temperatures and prolonged solvent treatment times enhanced lignin solubilization in both treatments. Elevating the temperature from 100 to 195°C in an ethanol-water mixture produced higher lignin yields from candlenut shells. The elevation in temperature promotes depolymerization, recondensation, and additional breakdown, resulting in enhanced amounts of lignin-derived phenols and unwanted byproducts. They also increase the likelihood of degrading the cellulosic fraction (Kumar et al. 2017). Likewise, extended exposure to extraction problems promotes lignin breakdown, whereas excessive treatment times may damage the cellulose (Kumar et al. 2017). Jiang et al. (2019) revealed that improving dilute NaOH pretreatment at moderate temperatures can result in high lignin removal, with maximum efficiency obtained under particular conditions. Specific factors must be carefully optimized to increase lignin production in these treatments to obtain the maximum amount of lignin. At the same time, the integrity of the cellulose is preserved.

This study employed alkaline and organosolv treatments to extract lignin from coconut pith (CP). Critical process parameters, including temperature, solvent concentration, and treatment time, were optimized using Design Expert's Response Surface Methodology (RSM) and Central Composite Design (CCD). The extracted lignin samples were subsequently characterized to assess their physicochemical properties using Fourier-transform infrared spectroscopy (FTIR) and thermogravimetric analysis (TGA). These methods provide a comprehensive understanding of lignin extraction and quality, supporting

its potential application in sustainable biorefinery processes.

METHODOLOGY

CHEMICALS AND MATERIALS

CP was purchased from HTC Coconut Sdn. Bhd in Teluk Intan, Perak. The chemicals utilized in this study for the extraction processes were sodium hydroxide (15% w/v, R&M Chemicals) and ethanol (70% w/v, Systerm Chemicals). Furthermore, sulfuric acid (H_2SO_4, 98%, Merck), dimethylsulfoxide (DMSO-d6, 99.96%, Sigma-Aldrich) were used. All chemicals and reagents used in this study, along with their purity and source, are listed in Table 1.

TABLE 1. The list of chemicals and reagents

Substance	Purity/ Concentration	Supplier/ Source
Coconut pith (CP)	-	HTC Coconut Sdn. Bhd, Teluk Intan, Perak
Sodium hydroxide, NaOH	15% w/v	R&M Chemicals
Ethanol	70% w/v	Systerm Chemicals
Sulfuric acid (H_2SO_4)	98%,	Merck
Hydrochloric acid (HCl)	37%,	Synth
Dimethylsulfoxide (DMSO-d6)	99.96%,	Sigma-Aldrich),

The proximate composition analysis of the CP that was analysed by the National Renewable Energy Laboratory (NREL) procedure found that CP contains cellulose (90.37%), hemicellulose (10.56%), lignin (41.26%), extractives (11.19%), other components (4.64%), and moisture (12.56%).

THE PREPARATION OF COCONUT PITH

The sample was washed well to get rid of any remaining impurities. It was then dried in an oven (UF 110, Memmert) at 50°C until the weight remained constant. Using a biomass grinder mill, the sample was dried and then ground by biomass grinder (SM 100, RETSCH) into particles about 0.2 mm in size. It was then sieved through a 40-mesh testing siever (AS 450, RETSCH). The extractions were done with a Soxhlet apparatus.

THE EXTRACTION TREATMENT

Alkaline treatment (AT) and organosolv treatment (OT) were performed in a round-bottom flask under reflux conditions at the solid-to-liquid ratio of 1:15% (w/v) and stirring at 400 rpm continuously.

For the organosolv treatment, ethanol solutions of desired concentrations were prepared by mixing ethanol with distilled water, following the method described by (Fan et al. 2022). CP powder was added into the ethanol solution in a round bottom flask and heated simultaneously agitated at the desired temperature for a period. The liquor obtained was filtered and distilled in a distillation column, followed by acidification with H_2SO_4 until solutions turned into pH 2 to induce lignin precipitation. The precipitated lignin was filtered using vacuum filtration, washed with distilled water, and oven-dried at 50°C for 12 hours. The dried lignin was stored in a laboratory desiccator. The extracted lignin was denoted as CPL-OT. This organosolv treatment was repeated with different concentrations of ethanol solutions (50, 60 and 70 % (v/v)), at different temperatures (60, 90 and 120°C) and different times (60, 120, and 180 minutes).

For the alkaline treatment, NaOH was prepared by dissolving an appropriate mass of NaOH pellets in distilled water. CP powder was added to the NaOH solution, and the mixture was stirred at the desired temperature for a period in a round-bottom flask. After treatment, a black liquor of pH 12 was obtained. The black liquor was then filtered and acidified with H_2SO_4 until pH 2, and lignin precipitation was obtained. The precipitated lignin was filtered using vacuum filtration, washed with distilled water, and oven-dried at 50°C for 12 hours. The dried lignin was then stored in a laboratory desiccator. The extracted lignin was denoted as CPL-AT. The alkaline treatment was repeated with different concentrations of NaOH solutions (4, 6, and 8 wt.%), at various temperatures (60, 90, and 120°C), and for different durations (60, 120, and 180 minutes).

PERCENTAGE LIGNIN YIELD EXTRACTED BY GRAVIMETRIC METHOD

The percentage of the CPL yield was calculated using the gravimetric method as per Equation (1).

$$\text{Lignin (\%)} = \frac{L(100)}{S} \quad (1)$$

where L is the weight of the extracted lignin (g), and S is the weight of the dried sample (g).

DETERMINATION OF THE PURITY OF LIGNIN BY KLASON METHOD

The Klason method separated the biomass into acid-insoluble and acid-soluble lignin components. Approximately 100 mg of extractive-free CPL was precisely weighed and transferred to test tubes, where 1 ml of 72% sulfuric acid was added and properly mixed. The tubes were immersed in a water bath at 30°C for 60 minutes, stirring every 10 minutes. The samples were diluted to 4% sulfuric acid concentration by adding 28 g of distilled water and auto-claving at 121°C for 1 hour. Once the hydrolysates had cooled to room temperature, they were vacuum-filtered. The filtrates were placed in sample bottles for analysis, which should be done within six hours (or stored in the refrigerator for up to two weeks). After being rinsed with around 50 ml of distilled water, the solid residues were transferred into crucibles and dried at 105 °C until their weight remained constant. Equation (2) was used to determine the acid-insoluble lignin (AIL) after it had dried.

$$\text{AIL (\%)} = \frac{(\text{R} - \text{A}) \times 100}{300\ \text{mg}} \quad (2)$$

where AIL is the acid-insoluble lignin, R is the residue of AIL after drying (mg), and A is the weight of the ash residue after furnaced (mg).

The crucibles were burned in the furnace and heated at 575°C to obtain ash residue. The residue ash was weighed to determine the AIL. The filtrate was then analyzed using a UV-Vis spectrophotometer (Shimadzu 1800), with absorbance measured at wavelengths 200 to 800 nm. Acid-soluble lignin (ASL) was determined using Equations (3) and (4).

$$\text{C} = \frac{\text{A}}{110} \times \frac{\text{V}_{\text{final}}}{\text{V}_{\text{initial}}} \quad (3)$$

$$\text{ASL (\%)} = \frac{\text{CV}_{Total} \times 100}{1000 \times 300\text{mg}} \times 100 \quad (4)$$

where, C is the filtrate concentration (g/mL), A is the absorbance at 270 nm, 300 mg is the mass of the sample CP for the extraction, V_{final} is the final volume of the solution (mL), $V_{initial}$ is the initial volume of the solution (mL), ASL is the acid-soluble lignin, , and VTotal is the total filtrate volume (mL).

The Klason lignin (KL) was calculated by combining AIL and ASL using Equation (5).

$$\text{KL(\%)} = \text{AIL(\%)} + \text{ASL (\%)} \quad (5)$$

where, KL is the Klason lignin or the purity of the extracted CP lignin.

CHARACTERIZATION OF THE EXTRACTED LIGNIN

The extracted CPL-AT and CPL-OT were characterized using FTIR and TGA analyses to observe structural and compositional differences. The chemical structure and functional group changes for CPL-AT and CPL-OT were conducted using FTIR spectroscopy (Perkin Elmer Spectrum FT-IR Spectrometer, Universal ATR). 1 mg of CPL samples were mixed with 100 mg KBr, then pressed into disks at 10 MPa for 3 minutes and properly ground before analysis. The spectra were obtained with an average of 25 scans and a resolution of 4 cm^{-1} in the 4000–400 cm^{-1} range (Su et al. 2022). CPL-AT and CPL-OT thermal stability were evaluated using a TG analyzer (TGA/DSC3+, Mettler Toledo, Switzerland). The test was performed by heating about 8 mg of extracted lignin from 35 to 800°C at 10°C/min under nitrogen at a 20 mL/min flow rate (Fan et al. 2022).

EXPERIMENTAL DESIGN OF THE BEST TREATMENT

A three-factor CCD was employed to identify the optimal extraction parameters for the best treatment. The design and optimization studies used Design Expert 13.0 statistical software to measure the lignin yield and purity using the regression model given in Equations (6) and (7), respectively.

$$\begin{aligned}\text{Y(Lignin yield)} = {} & \beta_0\text{(Intercept)} \\ & + \beta_1\text{A} + \beta_2\text{B} + \beta_3\text{C} \\ & + \beta_{11}\text{A}^2 + \beta_{22}\text{B}^2 \\ & + \beta_{33}\text{C}^2 + \beta_{12}AB \\ & + \beta_{13}AC + \beta_{23}BC\end{aligned} \quad (6)$$

$$\begin{aligned}\text{Y(Lignin purity)} = {} & \beta_0\text{(Intercept)} \\ & + \beta_1\text{A} + \beta_2\text{B} + \beta_3\text{C} \\ & + \beta_{11}\text{A}^2 + \beta_{22}\text{B}^2 \\ & + \beta_{33}\text{C}^2 \\ & + \beta_{12}\text{AB} + \beta_{13}\text{AC} \\ & + \beta_{23}\text{BC}\end{aligned} \quad (7)$$

where *Y* denotes the response value, whereas the β values in these models represent the regression coefficients corresponding to each term. β_0 represent intercept, β_1, β_2, β_3 denotes as linear effects of the independent variables (A

= temperature, B = solvent concentration, C = extraction time), β_{11}, β_{22}, β_{33} as quadratic effects and β_{12}, β_{13}, β_{23} as interaction effects between the variables.

These coefficients were calculated automatically by the software using least squares regression to fit the experimental data from the CCD. The significance of each β value was evaluated through ANOVA, which determines how strongly each factor and interaction influences lignin yield and purity. This approach allows prediction of the response values for any combination of temperature, solvent concentration, and extraction time within the studied ranges.

EXPERIMENTAL WORKFLOW

The overall experimental procedure followed a systematic sequence, as summarized in the flowchart in Figure 1.

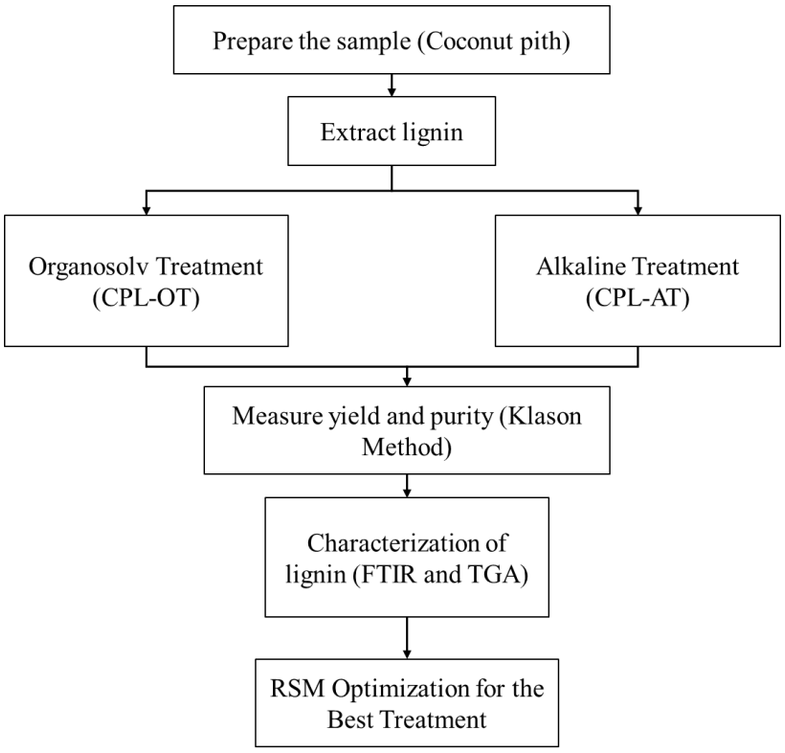

FIGURE 1. The flowchart of the overall experimental

RESULT AND DISSCUSSION

DETERMINATION OF THE PURITY OF LIGNIN BY KLASON METHOD

The Klason method separated the biomass into acid-insoluble and acid-soluble lignin components. Approximately 100 mg of extractive-free CPL was precisely weighed and transferred to test tubes, where 1 ml of 72% sulfuric acid was added and properly mixed. The tubes were immersed in a water bath at 30°C for 60 minutes, stirring every 10 minutes. The samples were diluted to 4% H_2S concentration by adding 28 g of distilled water and auto-claving at 121°C for 1 hour. Once the hydrolysates had cooled to room temperature, they were vacuum-filtered. The filtrates were placed in sample bottles for analysis, which should be done within six hours (or stored in the refrigerator for up to two weeks). After being rinsed with around 50 ml of distilled water, the solid residues were transferred into crucibles and dried at 105 °C until their weight remained constant. Equation (2) was used to determine the acid-insoluble lignin (AIL) after it had dried.

SCREENING OF THE ORGANOSOLV TREATMENT AND ALKALINE TREATMENT AT DIFFERENT PARAMETERS

This preliminary experiment was done before the optimization process to determine the range of parameters of temperature, time, and concentration for yield and purity of lignin extracted from AT and OT. AT and OT range reaction duration, extraction temperature, and solvent

concentration were based on optimal parameters from previous studies on lignin extraction from sugarcane bagasse and wheat straw (Arslan et al. 2020; Bergrath et al. 2023; Chotirotsukon et al. 2023; X. Li et al. 2018; Lirong et al. 2012; Nguyen-Thi et al. 2024; Nitsos et al. 2016; Wildschut et al. 2013; Wunna et al. 2017). The selected parameter ranges effectively maximized lignin yield and purity in comparable biomass sources, although these studies were not focused on CP. The same basis will be applied for studies at the same solid/liquid ratio of 1:15 % (w/v).

INFLUENCE OF THE REACTION TIME.

Figures 2(a) and 2(b) show the effect of the yield and purity of CPL at different reaction times for AT and OT, respectively, at a constant 1:15 % (w/v) of the solid/liquid ratio at different temperatures, concentrations, and times. Figure 1a shows that AT was enhanced by extending the reaction time to 180 minutes at 120°C of 4% NaOH, producing 60.75% of CPL-AT. Khaleghipour et al. (2021) discovered that repeated extraction with NaOH at increasing temperatures solubilized more lignin from sugarcane bagasse, demonstrating that extended exposure to NaOH can result in more effective lignin extraction. However, Miao et al. (2014) reported that the lignin content in natural sugarcane bagasse decreased from 25wt% to 17wt.% after mild AT with 2% NaOH at 120°C for 60 minutes. Lignin extraction yield and purity may be reduced when the reaction time exceeds 120 minutes, as some lignin remains.

However, Figure 2(b) for OT at 170 °C with 70 % (v/v) of ethanol shows that the production of CPL-OT decreases from 7.88% to 2.49% with the prolonged time of 180 minutes. It same goes with the CPL-OT purity. This indicates that a higher time of AT can improve the dissolution of CPL, leading to a more effective extraction process, while OT is vice versa. Nitsos et al. (2016) and Lawther et al. (1996) also mentioned that AT from different biomass produced a higher lignin yield than OT. The NaOH solution in AT dissolves the lignin fragments by ionizing aliphatic hydroxyls and phenolic groups, accelerating yield (Nasrun et al. 2023).

INFLUENCE OF THE EXTRACTION TEMPERATURE.

Figures 3(a) and 3(b) demonstrate the AT and OT extraction temperature, respectively, at a constant 1:15 % (w/v) of the solid/liquid ratio, concentration, and time. Figure 3(a), the extraction yield of CPL-AT increased to 55.93wt.% at 150°C using 2wt.% NaOH. Ma et al. (2021) study supported this increase in AT temperature for lignin yield. The research demonstrates that NaOH's effectiveness in solubilizing and fragmenting the lignin increases as the temperature reaction rises. However, Z. Zhang et al. (2021) illustrate that increased temperatures during AT may compromise the efficiency of lignin extraction. At high temperatures, the fragmentation of ether bonds and CPL-AT will be disrupted, causing the degradation of extracted CPL-AT and the formation of new compounds. Therefore, the optimal temperature range must be applied to extract the CPL-AT to hinder this phenomenon.

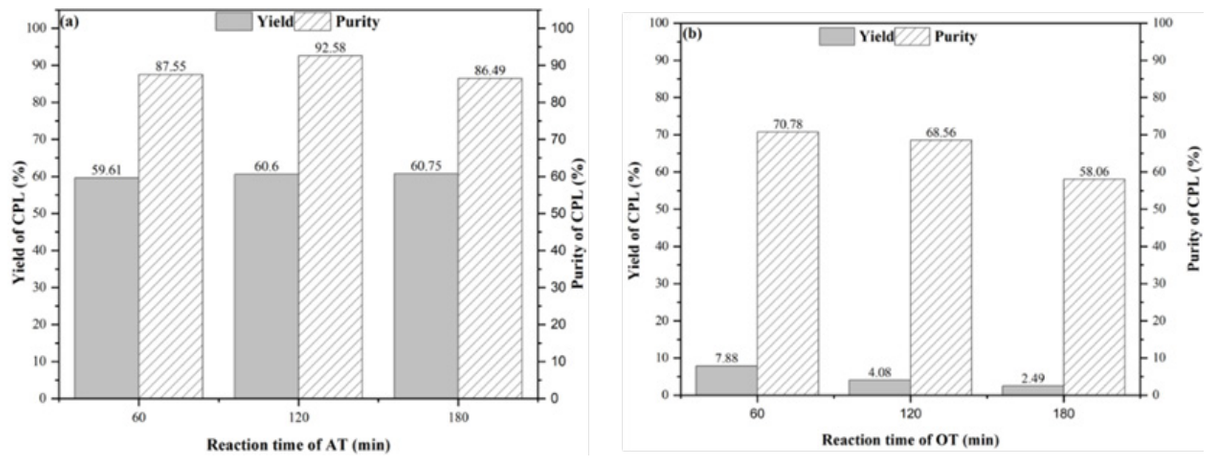

FIGURE 2. Effect of reaction time on (a) AT and (b) OT processes at constant solid/liquid ratio of 1:15 % (w/v), with fixed concentration and temperature.

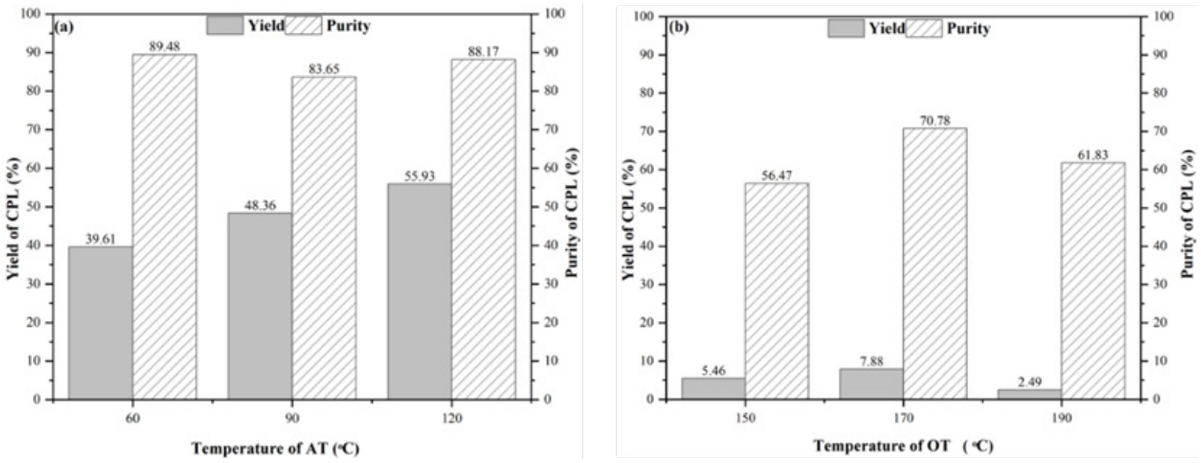

FIGURE 3. Effect of reaction temperature on (a) AT and (b) OT processes at constant solid/liquid ratio of 1:15 % (w/v), with fixed concentration and time.

Similarly, with the OT, as shown in Figure 3(b), increasing the temperature from 150°C to 190°C will decrease the CPL-OT yield from 5.46 to 2.99% at the concentration of ethanol 70%(v/v) for 60 minutes. However, at 170°C, the lignin yield and purity are at the highest values which means that that condition is the optimal condition for OT. Increasing the temperature in OT reduces CPL-OT yield due to thermal degradation, re-condensation with other components, and increased solubility of CPL-OT with the solvent, which prevents CPL-OT from fully precipitating during cooling. The higher temperatures also lead to by-product formation, incorporating CPL-OT fragments lost from the recoverable yield.

INFLUENCE OF THE SOLVENT CONCENTRATION.

The effect of NaOH concentration in AT and OT at constant 1:15 % (w/v) of the solid/liquid ratio, concentration, and temperature are illustrated in Figures 4(a) and 3(b). As illustrated in Figure 4(a), the AT yield the highest yield and purity which is at 60.75% and 83.01% respectively, at a lower concentration of NaOH and a peak yield of 2wt.%. Nevertheless, when the NaOH concentration went beyond 4wt.%, there was a marked reduction in the yield of CPL-AT extraction. Several studies also show that as the concentration of AT increases, the lignin production will also decrease (Huang et al. 2019) and (Chen et al. 2015) reported that increasing the NaOH concentration from 1 % to 5 % decreases the AT yielded from 22.5% to 18.3% for corn stover and wheat straw, respectively. These findings show that increased alkaline concentration can reduce the lignin yield due to the disruption of lignin and ether bonds and form new compounds.

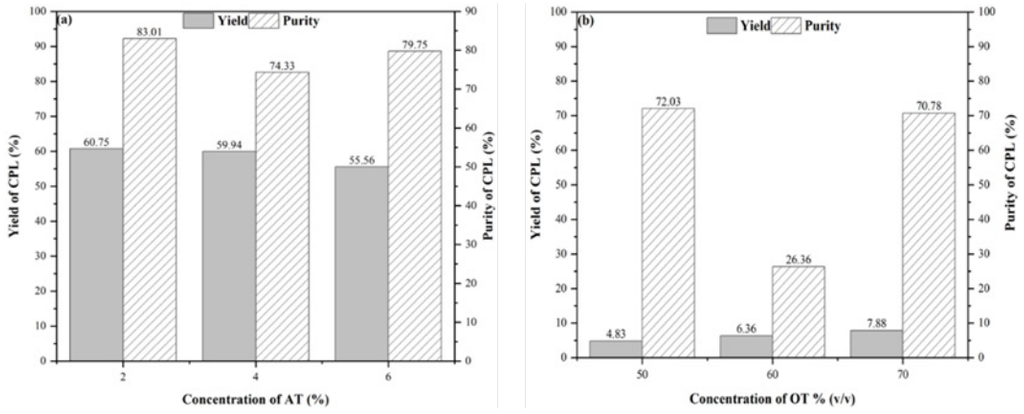

FIGURE 4. Effect of reaction concentration on (a) AT and (b) OT processes at constant solid/liquid ratio of 1:15 % (w/v), with fixed time and temperature.

For OT, as illustrated in Figure 4(b), increasing ethanol concentration from 50 to 70% (v/v) enhanced the CPL-OT yield to 7.88% due to improved solubilization. Ethanol is an organic solvent with the ability and strong affinity to interact with CPL-OT due to its aromatic and polar functional groups. The CPL-OT extracted from ethanol will remain more stable in the dissolved state at high solvent concentrations, reducing the chance of re-precipitation upon cooling. This helps maximize lignin yield during the extraction process (Tao et al. 2016). Adamcyk et al. (2023) indicated that the increases in ethanol concentration in lignin recovery from wheat straw and hardwood increase the dissolution rate of lignin by breaking down lignocellulosic structures more effectively. El Hage et al. (2010) found that the lignin extracted from Miscanthus and eucalyptus shows that greater treatment severity increases lignin's phenolic content, aiding extraction.

THE SCREENING OF YIELD AND PURITY OF CPL-AT AND CPL-OT.

Figure 5 compares CPL yield and purity of AT and OT at 1:15 % (w/v) with a constant 1:15 solid/liquid ratio % (w/v) but different parameters. The AT yielded the most CPL, 60.75%, with 86.49% purity, whereas the OT yielded just 7.88% of CPL, with 70.78% purity. This shows that AT generates a higher yield and purity of CPL with the respective condition treatments studied. Meanwhile, OT selectively produces a lower CPL yield and moderate CPL quality than AT. The purity of CPL-OT is still higher at low yields as they use milder, selective dissolution conditions that focus on purity over yield. This treatment only dissolves specific CPL-OT fractions, and reprecipitation happens as the solution cools. The low molecular weight of CPL-OT can easily alter the CPL-OT structure, making it more soluble but reducing overall recovery. Abd. Latiff also indicated that organosolv lignin's low molecular weight can still be preferable to specific applications since CPL is ideal for AT. Figure 5 shows that the purity of CPL-AT produced is higher (86.49%) than CPL-OT (70.78%). These conditions may be due to the low content of ash and large amounts of elemental sugars in CPL-OT that have been removed from acid washing. Nevertheless, the purity of CPL-OT can be increased more than CPL-AT through impurity removal. Further modifications of OT may aid in optimizing the production and purity of lignin to meet various industrial needs (Nitsos et al. 2016).

Additionally, the comparatively low CPL yield obtained from OT may be attributed to the absence of acid catalysis and the solvent–biomass ratio employed in this study. Organosolv delignification efficiency is strongly influenced by the presence of acid catalysts, which promote lignin depolymerization and enhance solubilization. In this study, mild extraction conditions were used. As a result, ethanol–water solvent without an acid catalyst dissolves only part of the lignin, so the overall recovery is low. Therefore, OT was not optimized for maximum yield but for selective extraction and better lignin quality. Increasing solvent severity or adding acid catalysts could increase the yield, but this would also increase chemical usage and reduce the environmental advantage of OT.

SURFACE CHEMISTRY ANALYSIS

Figure 6 presents the assignment and FTIR spectrum of CPL-AT and CPL-OT, highlighting key structural differences that reflect the influence of extraction conditions on the chemical composition of lignin. A broad absorption band in the region of 3400–3300 cm^{-1} is observed in both samples, corresponding to the O–H stretching vibrations of phenolic and aliphatic hydroxyl groups. This peak is more intense in CPL-OT, suggesting a higher concentration of free hydroxyl groups, which indicates reduced cleavage of ether

linkages (such as β-O-4) under the milder OT conditions. The preservation of these hydroxyl groups enhances CPL-OT's reactivity for downstream chemical modifications, particularly in applications like adhesives, coatings, and polymer synthesis (Paulsen Thoresen et al. 2021). In contrast, CPL-AT exhibits a weaker O–H stretching band, indicating a lower hydroxyl content due to partial cleavage of hydroxyl-bearing linkages, leading to a more condensed and thermally stable structure (Abd Latiff et al. 2022). Due to that, CPL-AT has a more condensed structure and provides lower reactivity, which will increase thermal stability and make it more suitable in filler applications in composite materials (Gao et al. 2019; Intapun et al. 2021).

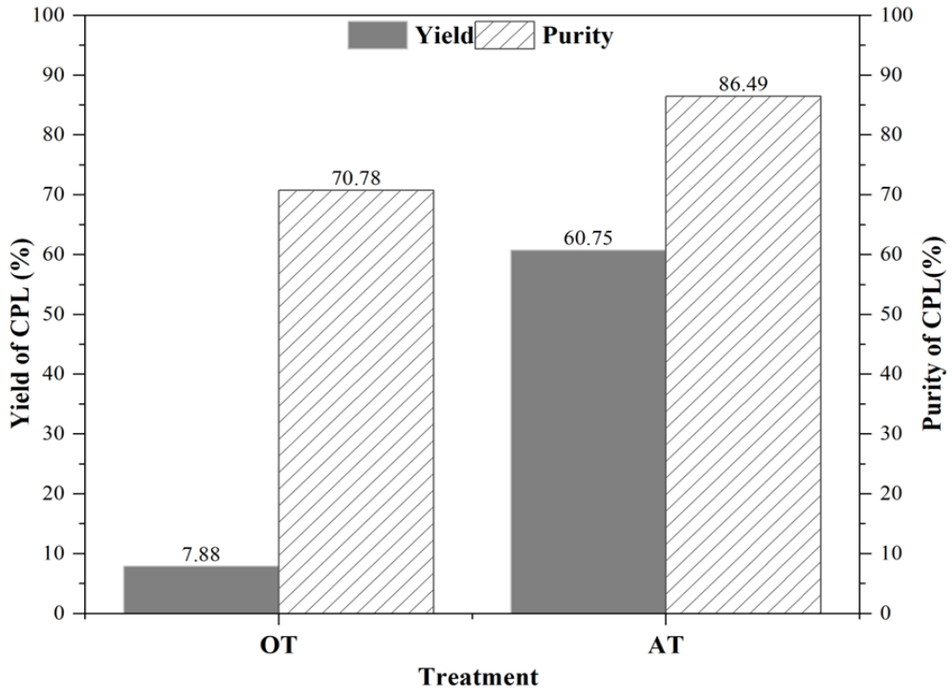

FIGURE 5. Comparison of CPL yield and purity of OT and AT at 1:15 % (w/v)

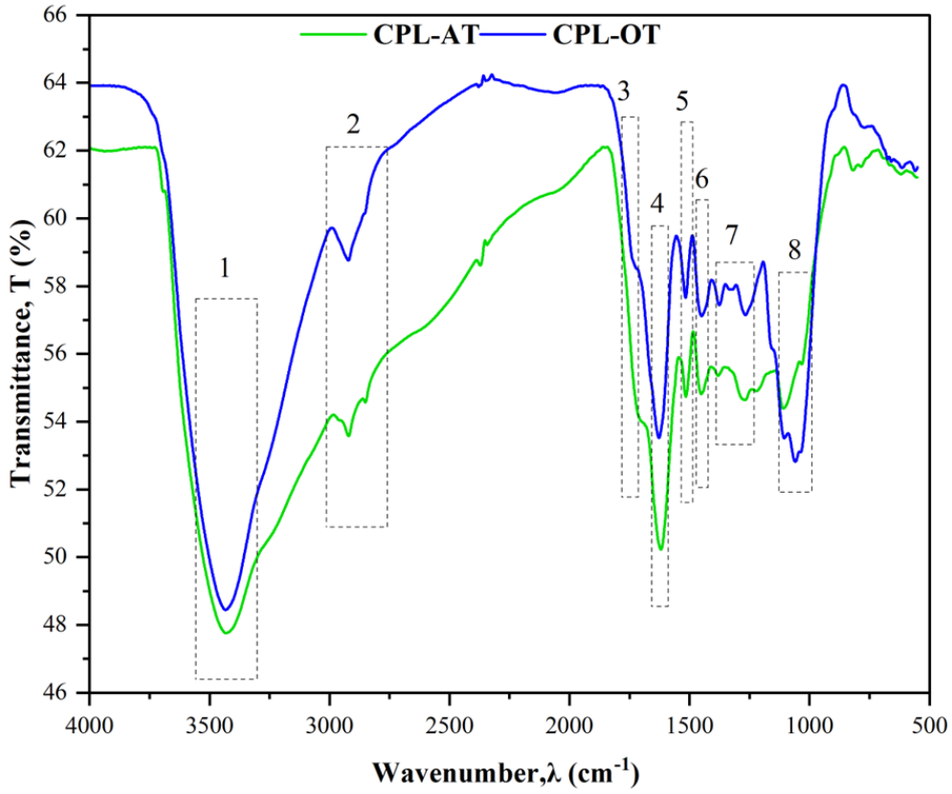

FIGURE 6 FTIR spectra of CPL

The absorption band around 2930–2850 cm^{-1}, attributed to C–H stretching in aliphatic chains, is more pronounced in CPL-OT, indicating better retention of aliphatic side chains. This structural trait contributes to CPL-OT's more complex and flexible architecture, which is beneficial for compatibility with hydrophobic matrices in polymer composites. The aliphatic side chains have a high amount in OL that contributes to a complex molecular structure and possibly increases compatibility with hydrophobic composite matrices (Sammons et al. 2013). The corresponding band in CPL-AT is significantly weaker, suggesting degradation of aliphatic components due to harsher extraction conditions in AT. This will also reduce CPL-AT reactivity and decrease CPL-AT volatility (P. Li et al. 2022). A distinct peak at 1710 cm^{-1} in the CPL-OT spectrum corresponds to the C=O stretching of unconjugated carbonyl groups such as ketones or esters. The presence of these functional groups enhances CPL-OT's potential for further chemical reactions and applications in reactive biobased materials(Jõul et al. 2022). In comparison, CPL-AT shows a lower-intensity peak in this region, implying fewer carbonyl functionalities and a more stable, less reactive polymeric framework. However, it shows a weaker peak for CPL-AT, but it is advantageous as this carbonyl can promote the degradation of CPL-AT (Lu et al. 2017). Both CPL samples display aromatic skeletal vibrations near 1600 and 1515 cm^{-1}, attributed to the C=C stretching of lignin's phenylpropanoid units. These peaks are sharper and more defined in CPL-OT, suggesting greater preservation of the aromatic backbone (Abd Latiff et al. 2022). This whole aromatic network may benefit applications where aromaticity is valued, such as carbon fiber precursors or UV-absorbing compounds.

CPL-OT also exhibits higher-intensity signals at 1450 and 1420 cm^{-1}, corresponding to C–H deformations in methyl, methylene, and methoxyl groups, further supporting the retention of lignin's native aliphatic and aromatic structures showing that benefit resins and thermosetting polymers (Podkościelna et al. 2015). These features are diminished in CPL-AT, indicating increased degradation of side chains. Still, CPL-AT has a lower intensity as AT degrades more aliphatic chain. The bands in the range of 1125–1110 cm^{-1} reflect the presence of guaiacyl (G) and syringyl (S) units, essential structural motifs in lignin (Hosseinaei et al. 2016; Lawther et al. 1996). CPL-OT displays more intense G and S signals, pointing to a higher syringyl content and a lower degree of condensation (Sammons et al. 2013).This structural feature imparts improved flexibility and processability, advantageous for producing coatings and films. CPL-AT, by contrast, shows reduced intensity in this region, indicating a more condensed structure with a lower content of syringyl units. Finally, ether linkages (C–O–C) between aromatic rings are evidenced by peaks around 1029–1059 cm^{-1}. These peaks are more prominent in CPL-OT, suggesting that the lignin structure remains more native and less disrupted under OT conditions (Karlsson et al. 2023). The reduced intensity of these bands in CPL-AT confirms greater cleavage of ether linkages during extraction, which leads to a lower molecular weight and more condensed structure which will make it more soluble in aqueous environments, making it suitable as a dispersant or stabilizer (Ouyang et al. 2009).

THERMAL STABILITY ANALYSIS

Figures 7(a) and 7(b) illustrate and tabulated the thermogravimetric analysis (TGA) values of CPL-OT and CPL-AT, offering detailed insights into their thermal stability and decomposition profiles. The TGA curves reveal two main stages of weight loss as temperature increases. The initial weight reduction occurs between 35°C and 150°C for both samples and is attributed primarily to the evaporation of physically adsorbed moisture and light volatiles (Huang et al. 2019). CPL-AT exhibits a weight loss of 15.08% in this phase, indicating greater moisture and volatile content compared to CPL-OT, which shows a smaller mass loss of 20.69% concentrated within a narrower low-temperature range (0–100°C), suggesting higher volatility and lower molecular weight (Chen et al. 2015).

The second major degradation phase is observed from approximately 150°C to 480°C, corresponding to the thermal decomposition of the lignin macromolecule. This stage involves the cleavage of ether bonds and degradation of side chains, leading to the formation of phenolic compounds, non-condensable gases, and char. CPL-OT begins significant mass loss at a lower onset temperature (~100°C) and reaches 50% weight loss at 541.92°C, indicating a more readily decomposable and less cross-linked structure. In contrast, CPL-AT begins substantial decomposition around 200°C and shows a slightly earlier 50% mass loss at 504.00°C, reflecting a more rigid and complex structure. The corresponding mass reductions in this phase are 26.79% for CPL-AT and 20.69% for CPL-OT, aligning with earlier findings by (Adamcyk et al. 2023) and (El Hage et al. 2010), who reported lignin degradation typically occurs between 200°C and 540°C.

At 600°C, CPL-OT retains a higher residual mass of 44.46% compared to 39.23% for CPL-AT. This higher char yield in CPL-OT suggests better thermal resistance and a more stable carbonaceous backbone. The maximum degradation rate temperature (DTG_{max}) is recorded at 795.76°C for CPL-OT and 797.40°C for CPL-AT, indicating that both samples exhibit their peak decomposition

near 800°C. Beyond this point, both materials enter a slow degradation phase associated with carbon restructuring and ash formation. Overall, CPL-OT demonstrates moderately higher thermal stability and residue retention than CPL-AT, likely due to its less condensed and more thermally responsive structure. These characteristics are important when evaluating lignin's suitability for thermally demanding applications, such as polymer composites, adhesives, and biocarbon materials (Choi et al. 2021). On the other hand, CPL-AT's more excellent thermal stability up to 200°C implies potential for applications requiring heat resistance, such as high-temperature resins or composites (Y. Zhang et al. 2017).

RESPONSE SURFACE METHODOLOGY (RSM)

In this study, response surface methodology (RSM) with central composite design (CCD) was employed to optimize the alkaline treatment (AT) process parameters such as temperature, NaOH concentration, and reaction time with a constant solid-to-liquid ratio of 1:15 % (w/v).

AT was selected based on preliminary screening results, which showed that it produced significantly higher lignin yield and purity from AT compared to OT. CCD was chosen for its effectiveness in modeling quadratic responses and capturing interactions among variables with fewer experimental runs, thus minimizing time and cost. The coded levels and factor ranges used in the CCD, as presented in Table 2, were determined through initial screening to encompass conditions that maximize lignin extraction efficiency. This approach allowed for a detailed investigation into the effects and interactions of temperature, NaOH concentration, and reaction time on CPL-AT yield and purity.

TABLE 2. The Coding Levels for Variables That Influence Factors in The CCD Design

Variables	Factors	Coded levels		
		− 1	0	+ 1
Extraction temperature (°C)	A	90	120	150
Sodium Hydroxide solution concentration (wt.%)	B	4	6	8
Reaction time (min)	C	120	180	240

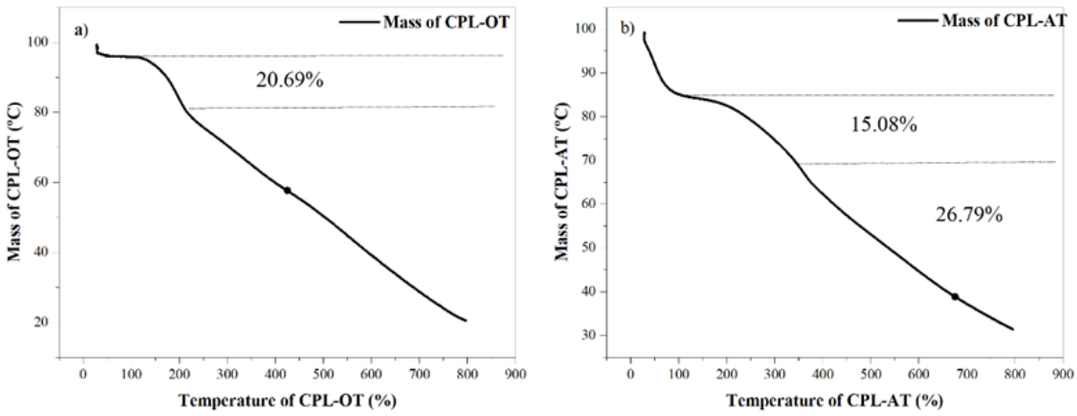

FIGURE 7. TGA graphs of combustion in (a) CPL-OT and (b) CPL-AT\

EXPERIMENTAL DESIGN

Table 2 tabulated the CCD model with coded forms of process variables and values of experimental data for AT. As shown in Table 2, each experimental run varied by one or more factor levels to capture the combined effect on CPL-AT yield and purity. The objective was to maximize both responses. The results indicated that CPL-AT contents ranged from 47.4% to 64.8% and purity from 78.4% to 86.0%. The highest CPL-AT was 64.8% and purity 80.0%, with treatment conditions of 150°C, 4wt.% NaOH concentration, and a 240-minute reaction time.

STATISTICAL ANALYSIS OF VARIANCE (ANOVA)

Statistical analysis for the regression model of lignin yield and lignin purity of CPL-AT using CCD is shown in Tables 3 and 4. As shown in Table 3, the F-value is statistically significant, with a strong F-value of 118.35 and a low p-value of less than 0.0001. This p-value, below the conventional significance threshold of 0.05, supports rejecting the null hypothesis and reveals the influence of the factor or interaction on the response variable. The lack of fit of the F-value indicates 2.84 values, which are significantly greater than 1, suggesting that the model is not significant in relative error. Therefore, the model has

a significant amount for the desirability. an insignificant value because the p-value is more than 0.05, presenting errors that do not affect the model. It also indicated that the value of correlation coefficient R^2 is 0.9907, which shows how well the data fit the regression model. It stated that the higher the R^2, the better the model fits the data (Imrana & Haruna, 2017). Adjusted R^2 of 0.9823 indicated it decreases as the predictor by less than expected by chance. It accounts for the model complexity and provides a more accurate picture of how well the model generalizes, mainly when multiple predictors exist. Predicted R^2 is a more direct measure of how well the model will work on unknown data. As shown in Table 3 for lignin purity, the F-value and p-value of 47.46 and < 0.0001, respectively. The lack of fit of F-value and p-value of 2.84 and 0.14, respectively demonstrated that the lack of fit of lignin purity is not significant relative to the pure error. The R^2 of the lignin purity are 0.9567, indicate that the models have a quite good agreement with the experimental data.

TABLE 3. ANOVA of Lignin Yield

Source	Sum of squares	Df	Mean square	F-value	p-value	
Model	504.96	9	56.11	118.35	< 0.0001	
A-Temperature	101.85	1	101.85	214.85	< 0.0001	significant
B-Concentration	34.95	1	34.95	73.72	< 0.0001	
C-Time	9.49	1	9.49	20.01	0.0012	
AB	16.79	1	16.79	35.42	0.0001	
AC	20.58	1	20.58	43.40	< 0.0001	
BC	11.45	1	11.45	24.15	0.0006	
A^2	89.20	1	89.20	188.14	< 0.0001	
B^2	29.89	1	29.89	63.05	< 0.0001	
C^2	235.82	1	235.82	497.42	< 0.0001	
Residual	4.74	10	0.4741		< 0.0001	
Lack of Fit	3.51	5	0.7014	2.84	0.1382	not significant
Pure Error	1.23	5	0.2468			
Cor Total	509.70	19				

TABLE 4. Fit Statistics

Standard deviation	0.6885	R^2	0.9907
Mean	53.09	Adjusted R^2	0.9823
Adeq precision	35.7160	Predicted R^2	0.9434

DIAGNOSTIC OF MODEL ADEQUACY

Figure 8(a) and Figure 8(c) demonstrate the percentage of normal probability plots of residuals for lignin yield and lignin purity respectively were scattered near along the straight line, which denotes the residuals are normally distributed. Figure 8(b) and Figure 8(d) present the accuracy of lignin yield and lignin purity respectively by comparing the predicted response values with actual values from the model to the precise. The points grouping near the 45-degree line, show that real and expected values are similar. However, if the model is a poor fit, some adjustments are required, such as adding or removing terms depending on what has been observed in the plot.

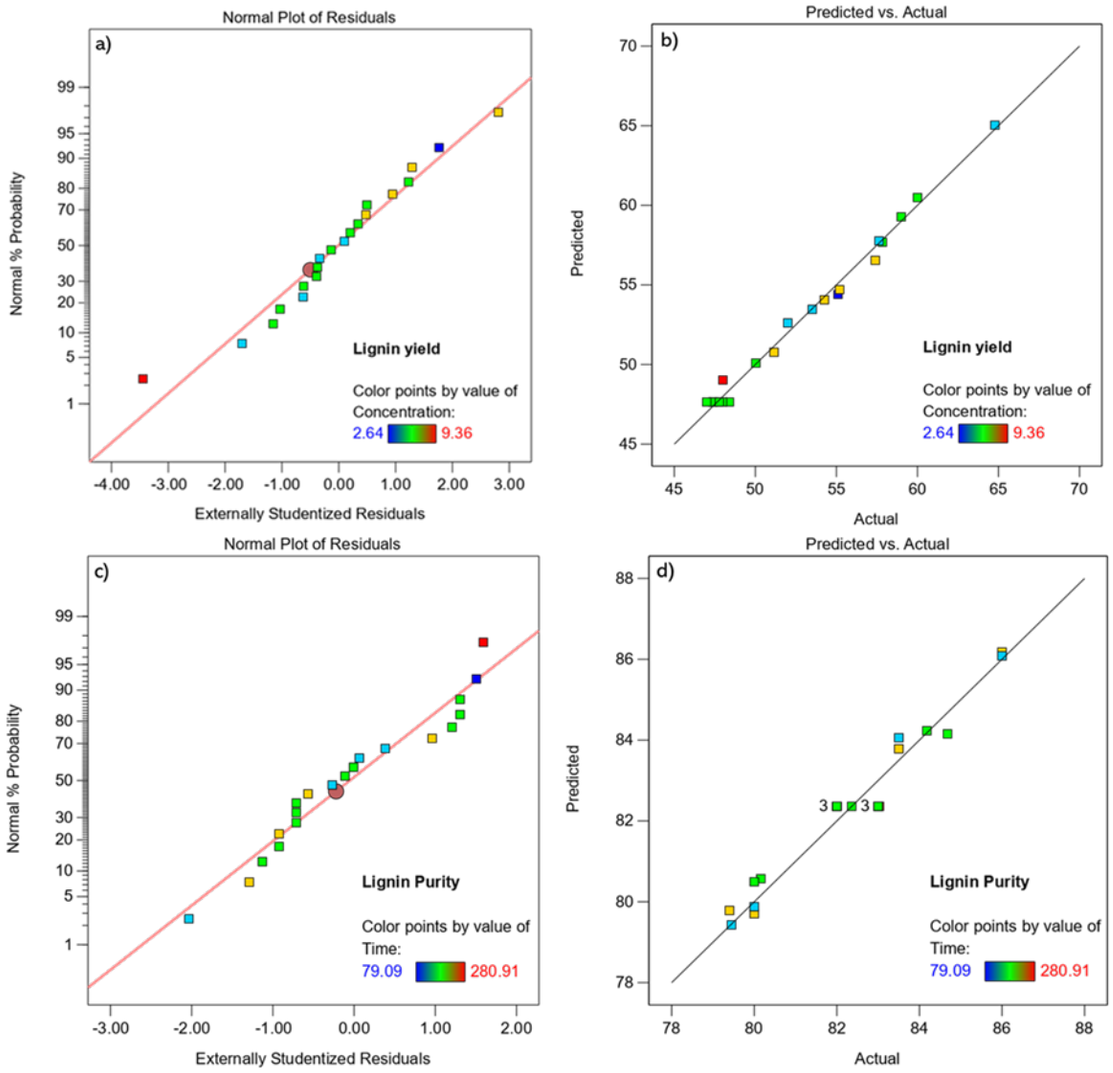

FIGURE 8. (a) Normal plot of residuals of lignin yields, (b) predicted versus actual lignin yields (c) Normal plot of residuals of lignin purity, (d) predicted versus actual lignin purity

FITTING MODELS

In this work, a second-order polynomial mathematical equation presented the relationship between the independent variables and the responses. The developed model equations for lignin yield and lignin purity were provided in Equations (8) and (9), where A, B, and C represent NaOH concentration (%), temperature (°C), and reaction time (min), respectively.

$$\begin{aligned}\text{Lignin yield (\%)} &= 47.65 + 4.59\,A \\ &- 2.69\,B - 1.40\,C \\ &- 4.09\,AB + 4.54\,AC \\ &- 3.38\,BC + 7.04\,A^2 \\ &+ 4.07\,B^2 + 11.44\,C^2\end{aligned} \tag{8}$$

$$\begin{aligned}\text{Lignin purity (\%)} &= 82.36 - 1.79\,A \\ &+ 1.87\,B + 0.0001\,C \\ &+ 1.75\,AB + 4.65\,AC \\ &+ 4.26\,BC\end{aligned} \tag{9}$$

THE EFFECT OF OPTIMIZATION OF VARIABLES

The interactions depicted in Figures 9(a-f) showed the 3D plots for the interaction lignin yield and purity, respectively between temperature and concentration (AB), temperature and time (AC), and concentration and time (BC), respectively. Figure 8(a) illustrates how the interaction of temperature (A) and concentration (B) effect the CPL-AT

yield. The higher temperature can lead to the solubilization of the CPL-AT, which will increase the CPL-AT, while the higher NaOH concentration decreases the CPL-AT yield. For instance, at 150 °C, the CPL-AT yield is high, around 60 %, at a lower concentration; as the concentration increases at the same temperature, the CPL-AT yield drops to 50 %.

Figure 9(b) shows the interaction of temperature (A) and time (C) effect the CPL-AT yield as the higher the treatment temperature and time, the higher the CP-AT yield. For instance, at the concentration 6wt.% and 120 °C, the CPL-AT yield is predicted to increase from 67 % to 80 % as the cooking time increases to 300 minutes. Over time, the rate of CPL-AT yield will eventually reach equilibrium, where the amount of AL being dissolved equals the amount that can be recovered. Before reaching this equilibrium, the yield will generally continue to increase. Figure 9(c) shows that the interaction of concentration (B) and time (C) effect the CPL-AT yield. The higher the concentration (B) of NaOH, the lower the CPL-AT yield contents meanwhile, the longer reaction time (C) results in a higher CPL-AT yield content. However, the longer the exposure time for the treatment process, the CPL-AT yield content starts to decrease. For example, at 4wt.% at 120°C, it requires a lower time to increase the CPL-AT yield to 60%, while at 9wt.%, the CPL-AT yield decreases as the time increases. The CPL-AT yield was predicted to drop at high concentrations as time increases.

The interactions depicted in Figure 9(d-f) showed the 3D plots for the interaction between the lignin purity and the temperature and concentration (AB), temperature and time (AC), and concentration and time (BC), respectively. Figure 9(d) illustrates how the interaction of temperature (A) and concentration (B) effect the CPL-AT purity at higher temperature increases the purity, while the higher NaOH concentration decreases the purity. Figure 8e shows the interaction of temperature (A) and time (C) increases the purity at higher temperature and time. Figure 9(f) shows that the interaction of concentration (B) and time (C) effect the CPL-AT purity as the higher the concentration (B) of NaOH and time (C), the lower the purity meanwhile, the longer reaction time (C) results in a higher CPL-AT yield content.

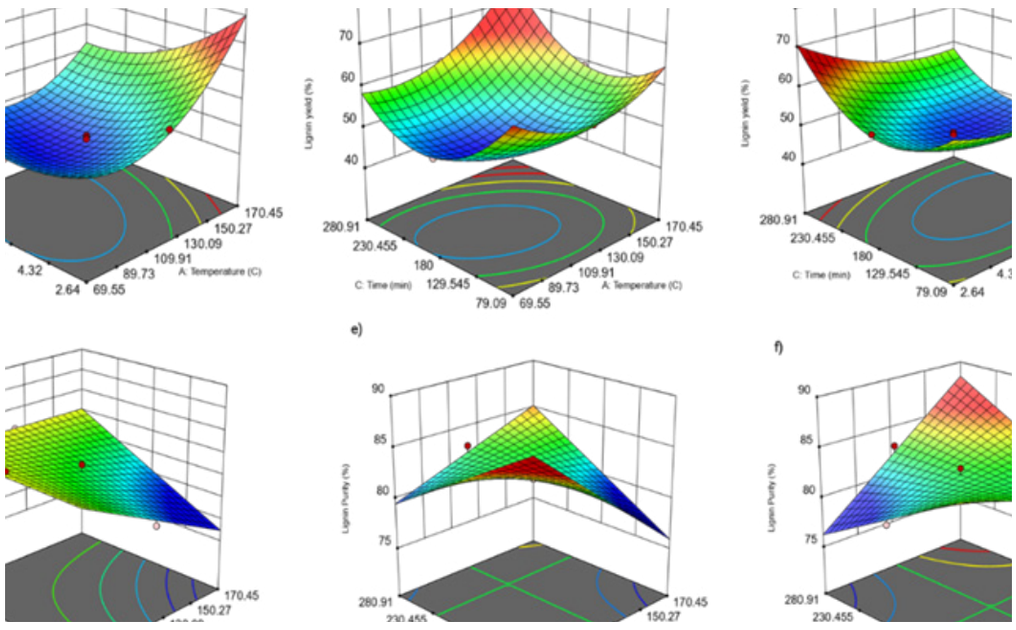

FIGURE 9. 3D response surface plots showing the effects of temperature (A), concentration (B), and time (C) on CPL-AT (a-c) yield and (d-f) purity, with contour projections highlighting parameter interactions

OPTIMIZATION CONSTRAINT FOR CPL-AT YIELD AND PURITY USING THE DESIRABILITY FUNCTION

Table 5 shows the optimization of constraint limit as to obtain the desired lignin yield and purity. The choice of the goal of optimization of the independent variables was based on the ANOVA while the goal of the dependent variables w ere based on the lignin extraction production. The result shows with the temperature of 150°C, NaOH concentration of 4wt%, and reaction time of 240 minutes are able to produce the most desired optimal result with yield of 65.04 and purity of 79.65%. To validate this predicted response, confirmatory runs were also performed.

It was observed that the predicted response employed an error between 5 to 13%. Overall, this low percent error incurred by the quadratic model strongly suggests that it could be used to accurately determine true values of the response variable within the working ranges specified in this study.

TABLE 5. Constraints limits and the optimal solution results

Name	Goal	Lower Limit	Upper Limit	Importance	Optimal result
A: Temperature (°C)	In range	69.55	170.45	3 (Important)	165.20
B: NaOH Concentration (wt.%)	In range	2.64	9.36	3 (Important)	6.59
C: Reaction Time (min)	In range	79.09	280.91	3 (Important)	278.64
Response 1: Lignin yield (wt.%)	Maximize	47	64.78	3 (Important)	72.29
Response 2: Purity of lignin (wt.%)	In range	78.4	86	3 (Important)	86.00

CONCLUSION

In conclusion, AT extracted the highest amount of CPL-AT from CP at % 60.75 % of lignin yield and 86.49% of lignin purity. In contrast, OT only produced a 15.94% yield of CPL-OT with 72.03% purity. The best conditions for AT, as found by RSM, are 278.64 minutes at 165.20°C with 6.59 wt.% NaOH and a solid-to-liquid ratio of 1:15 % (w/v). The CPL-AT produced 72.29% of lignin yield with a purity of 86.00% under these optimal conditions, per the expected results. FTIR analysis demonstrated that CPL-AT and CPL-OT possess similar spectrums, though the CPL-OT showed more prominent peaks of aromatic rings and phenolic hydroxyl groups. However, TGA studies demonstrated that CPL-AT has higher heat stability owing to its higher molecular weight and solubility properties. CPL-AT's high purity and production indicate many possible uses and advantages over other sources or extraction methods, and it is suitable for CPL extraction. CPL-AT's exceptional thermal stability and solubility can be used as raw or additive materials to produce bio-based polymers, adhesives, and composites. At the same time, its molecular weight and structure are advantageous for further chemical modification and applications like carbon fibers, fuel additives, and bioplastics. With these attributes, CPL-AT can be further processed as a viable and beneficial product for use in the industry with the improvement of treatment results for three crucial process variables and their characterization of the physicochemical properties.

ACKNOWLEDGEMENT

The author gratefully acknowledges the financial support from the Yayasan Universiti Teknologi Petronas Fundamental Research Grant (YUTP-FRG) under cost center 015LC0-459.

DECLARATION OF COMPETING INTEREST

None.

REFERENCES

Abd Latiff, N. H., Brosse, N., Ziegler-Devin, I., Chrusiel, L., Hashim, R. & Hussin, M. H. 2022. A comparison of alkaline and organosolv lignin extraction methods from coconut husks as an alternative material for green applications. *BioResources* 17(1): 469–491.

Adamcyk, J., Beisl, S. & Friedl, A. 2023. High temperature lignin separation for improved yields in ethanol organosolv pre-treatment. *Sustainability* 15(4): 3006. https://doi.org/10.3390/su15043006

Anuchi, S. O., Hallett, J. P. & Campbell, K. L. S. 2022. *Ionic Liquid-Assisted Process: Biomass-Derived Carbonaceous Materials*. Imperial College London.

Anuchi, S. O., Sedransk Campbell, K. L. & Hallett, J. P. 2022. Effective pretreatment of lignin-rich coconut wastes using a low-cost ionic liquid. *Scientific Reports* 12(1). https://doi.org/10.1038/s41598-022-09629-4

Arslan, C., Javed, M., Sattar, A., Ilyas, F., Tariq, W. & Gillani, S. H. 2020. Optimizing the effect of chemical pretreatment on lignocellulosic properties of wheat straw. *Journal of Wastes and Biomass Management* 2(2): 28–32. https://doi.org/10.26480/jwbm.02.2020.28.32

Bajwa, D. S., Pourhashem, G., Ullah, A. H. & Bajwa, S. G. 2019. A concise review of current lignin production, applications, products and their environment impact.

Industrial Crops and Products 139: 111526. https://doi.org/10.1016/j.indcrop.2019.111526

Bali, G., Meng, X., Deneff, J. I., Sun, Q. & Ragauskas, A. J. 2015. The effect of alkaline pretreatment methods on cellulose structure and accessibility. *ChemSusChem* 8(2): 275–279. https://doi.org/10.1002/cssc.201402752

Bergrath, J., Rumpf, J., Burger, R., Do, X. T., Wirtz, M. & Schulze, M. 2023. Beyond yield optimization: The impact of organosolv process parameters on lignin structure. *Macromolecular Materials and Engineering* 308(10): 2300093. https://doi.org/10.1002/mame.202300093

Chen, H., Zhao, J., Hu, T., Zhao, X. & Liu, D. 2015. A comparison of several organosolv pretreatments for improving the enzymatic hydrolysis of wheat straw: Substrate digestibility, fermentability and structural features. *Applied Energy* 150: 224–232. https://doi.org/10.1016/j.apenergy.2015.04.030

Choi, J. H., Cho, S. M., Kim, J. C., Park, S. W., Cho, Y. M., Koo, B., Kwak, H. W. & Choi, I. G. 2021. Thermal properties of ethanol organosolv lignin depending on its structure. *ACS Omega* 6(2): 1534–1546. https://doi.org/10.1021/acsomega.0c05234

Chotirotsukon, C., Jirachavala, K., Raita, M., Pongchaiphol, S., Hararak, B., Laosiripojana, N. & Champreda, V. 2023. Effects of thermal and physical modification on functional properties of organosolv lignin from sugarcane bagasse and its application in cosmeceutical products. *Frontiers in Chemical Engineering* 5. https://doi.org/10.3389/fceng.2023.1099010

El Hage, R., Brosse, N., Sannigrahi, P. & Ragauskas, A. 2010. Effects of process severity on the chemical structure of *Miscanthus* ethanol organosolv lignin. *Polymer Degradation and Stability* 95(6): 997–1003. https://doi.org/10.1016/j.polymdegradstab.2010.03.012

Espinoza-Acosta, J. L., Torres-Chávez, P. I., Olmedo-Martínez, J. L., Vega-Rios, A., Flores-Gallardo, S. & Zaragoza-Contreras, E. A. 2018. Lignin in storage and renewable energy applications: A review. *Journal of Energy Chemistry* 27(5): 1422–1438. https://doi.org/10.1016/j.jechem.2018.02.015

Fan, J., Yu, Q., Li, M., Chen, J., Wang, Y., Zhang, Y., Li, G., Ma, X., Zhong, H. & Yu, Y. 2022. Optimization of ethanol-extracted lignin from palm fiber by response surface methodology and preparation of activated carbon fiber for dehumidification. *Bioresources and Bioprocessing* 9(1). https://doi.org/10.1186/s40643-022-00549-9

Gao, Y., Qu, W., Liu, Y., Hu, H., Cochran, E. & Bai, X. 2019. Agricultural residue-derived lignin as the filler of polylactic acid composites and the effect of lignin purity on the composite performance. *Journal of Applied Polymer Science* 136(35): 47915. https://doi.org/10.1002/app.47915

Hosseinaei, O., Harper, D. P., Bozell, J. J. & Rials, T. G. 2016. Role of physicochemical structure of organosolv hardwood and herbaceous lignins on carbon fiber performance. *ACS Sustainable Chemistry & Engineering* 4(10): 5785–5798. https://doi.org/10.1021/acssuschemeng.6b01828

Huang, J., Liu, Y., Sun, B., Li, J., Zhang, R. & Nie, S. 2019. Laccase pretreatment for enhancing microwave-assisted alkaline extraction of hemicellulose from bagasse. *BioResources*.

Imrana, A. & Haruna, V. 2017. Geology, mineralogy and geochemistry of Koton-Karfe oolitic iron ore deposit, Bida Basin, Kogi State, Nigeria. *International Journal of Scientific & Technology Research*. www.ijstr.org

Intapun, J., Rungruang, T., Suchat, S., Cherdchim, B. & Hiziroglu, S. 2021. The characteristics of natural rubber composites with klason lignin as a green reinforcing filler: Thermal stability, mechanical and dynamical properties. *Polymers* 13(7): 1109. https://doi.org/10.3390/polym13071109

Jiang, K., Ding, S. & Tang, B. 2019. Optimization of dilute NaOH pretreatment at mild temperatures for monomeric sugar release from sorghum pith using response surface methodology. *BioResources* 14(2).

Jõul, P., Ho, T. T., Kallavus, U., Konist, A., Leiman, K., Salm, O. S., Kulp, M., Koel, M. & Lukk, T. 2022. Characterization of organosolv lignins and their application in the preparation of aerogels. *Materials* 15(8): 2861. https://doi.org/10.3390/ma15082861

Karlsson, M., Romson, J., Elder, T., Emmer, Å. & Lawoko, M. 2023. Lignin structure and reactivity in the organosolv process studied by NMR spectroscopy, mass spectrometry, and density functional theory. *Biomacromolecules* 24(5): 2314–2326. https://doi.org/10.1021/acs.biomac.3c00186

Kaur, R. 2015. Structural characterization and antioxidant activity of lignin from sugarcane bagasse. *Colloid and Polymer Science* 293(9): 2585–2592. https://doi.org/10.1007/s00396-015-3653-1

Khaleghipour, L., Linares-Pastén, J. A., Rashedi, H., Ranaei Siadat, S. O., Jasilionis, A., Al-Hamimi, S., Sardari, R. R. R. & Karlsson, E. N. 2021. Extraction of sugarcane bagasse arabinoxylan, integrated with enzymatic production of xylo-oligosaccharides and separation of cellulose. *Biotechnology for Biofuels* 14(1). https://doi.org/10.1186/s13068-021-01993-z

Kumar, A. K. & Sharma, S. 2017. Recent updates on different methods of pretreatment of lignocellulosic feedstocks: A review. *Bioresources and Bioprocessing* 4(1). https://doi.org/10.1186/s40643-017-0137-9

Lawther, J. M., Sun, R. C. & Banks, W. B. 1996. Characterization of dissolved lignins in two-stage organosolv delignification of wheat straw. *Journal of Wood Chemistry and Technology* 16(4): 439–457. https://doi.org/10.1080/02773819608545825

Li, P., Lu, Y., Li, X., Ren, J., Jiang, Z., Jiang, B. & Wu, W. 2022. Comparison of the degradation performance of seven different choline chloride-based DES systems on alkaline lignin. *Polymers* 14(23): 5100. https://doi.org/10.3390/polym14235100

Li, X., Luo, Y., Daroch, M., Hou, J. & Gui, W. 2018. Oxygen-assisted ethanol organosolv pretreatment of sugarcane bagasse for efficient removal of hemicellulose and lignin. *Cellulose* 25(10): 5511–5522. https://doi.org/10.1007/s10570-018-1960-7

Lin, Q., Yan, Y., Liu, X., He, B., Wang, X., Wang, X., Liu, C. & Ren, J. 2020. Production of xylooligosaccharide, nanolignin, and nanocellulose through a fractionation strategy of corncob for biomass valorization. *Industrial & Engineering Chemistry Research* 59(39): 17429–17439. https://doi.org/10.1021/acs.iecr.0c02161

Lirong, H., Feng, J., Zhang, S., Ma, Z., Wang, Y. & Zhang, X. 2012. Alkali pretreatment of wheat straw and its enzymatic hydrolysis. *Brazilian Journal of Microbiology*: 53–61.

Lu, Y., Lu, Y. C., Hu, H. Q., Xie, F. J., Wei, X. Y. & Fan, X. 2017. Structural characterization of lignin and its degradation products with spectroscopic methods. *Journal of Spectroscopy* 2017. https://doi.org/10.1155/2017/8951658

Ma, Z., Chen, S., Yin, Y., Zhou, Y., Lu, X. & Lin, T. 2021. Study on measurement model of lignin content in pulp after alkaline extraction. *Journal of Environmental Engineering and Landscape Management* 29(2): 94–100. https://doi.org/10.3846/jeelm.2021.14182

Miao, Q., Zhong, G., Qin, M., Chen, L. & Huang, L. 2014. Influence of alkaline treatment and alkaline peroxide bleaching of aspen chemithermomechanical pulp on dissolved and colloidal substances. *Industrial & Engineering Chemistry Research* 53(6): 2544–2548. https://doi.org/10.1021/ie4040785

Nasrun, Z., Osman, L. S., Latif, N. H. A., Elias, N. H. H., Saidin, M., Shahidan, S., Abdullah, S. H. A., Ali, N. A., Rusli, S. S. M., Ibrahim, M. N. M., Raja, P. B., Iqbal, M. A. M., Trache, D. & Hussin, M. H. 2023. Conversion of archeological iron rust employing coconut husk lignin. *International Journal of Biological Macromolecules* 253: 126786. https://doi.org/10.1016/j.ijbiomac.2023.126786

Nguyen-Thi, N. Y., Nguyen, C. Q., Le Dang, Q., De Tran, Q., Do-Thi, T. N. & Vu Thanh, L. H. 2024. Extracting lignin from sugarcane bagasse for methylene blue and hexavalent chromium adsorption in textile wastewater: A facile, green, and sustainable approach. *RSC Advances* 14(7): 4533–4542. https://doi.org/10.1039/d3ra08007b

Nitsos, C., Stoklosa, R., Karnaouri, A., Vörös, D., Lange, H., Hodge, D., Crestini, C., Rova, U. & Christakopoulos, P. 2016. Isolation and characterization of organosolv and alkaline lignins from hardwood and softwood biomass. *ACS Sustainable Chemistry & Engineering* 4(10): 5181–5193. https://doi.org/10.1021/acssuschemeng.6b01205

Ouyang, X., Ke, L., Qiu, X., Guo, Y. & Pang, Y. 2009. Sulfonation of alkali lignin and its potential use in dispersant for cement. *Journal of Dispersion Science and Technology* 30(1): 1–6. https://doi.org/10.1080/01932690802473560

Paulsen Thoresen, P., Lange, H., Crestini, C., Rova, U., Matsakas, L. & Christakopoulos, P. 2021. Characterization of organosolv birch lignins: Toward application-specific lignin production. *ACS Omega* 6(6): 4374–4385. https://doi.org/10.1021/acsomega.0c05719

Podkościelna, B., Sobiesiak, M., Zhao, Y., Gawdzik, B. & Sevastyanova, O. 2015. Preparation of lignin-containing porous microspheres through the copolymerization of lignin acrylate derivatives with styrene and divinylbenzene. *Holzforschung* 69(6): 769–776. https://doi.org/10.1515/hf-2014-0265

Sammons, R. J., Harper, D. P., Labbé, N., Bozell, J. J., Elder, T. & Rials, T. G. 2013. Characterization of organosolv lignins using thermal and FT-IR spectroscopic analysis. *BioResources* 8(2): 2752–2767.

Sand, A. & Tuteja, J. 2022. Lignin: Chemistry, structure, and application. In *Lignin: Chemistry, Structure, and Application*. IntechOpen. https://doi.org/10.5772/intechopen.102263

Singh, J., Suhag, M. & Dhaka, A. 2015. Augmented digestion of lignocellulose by steam explosion, acid and alkaline pretreatment methods: A review. *Carbohydrate Polymers* 117: 624–631. https://doi.org/10.1016/j.carbpol.2014.10.012

Souto, F., Calado, V. & Pereira, N. 2018. Lignin-based carbon fiber: A current overview. *Materials Research Express* 5(7). https://doi.org/10.1088/2053-1591/aaba00

Su, X., Fu, Y., Shao, Z., Qin, M., Li, X. & Zhang, F. 2022. Light-colored lignin isolated from poplar by ultrasound-assisted ethanol extraction: Structural features and anti-ultraviolet and anti-oxidation activities. *Industrial Crops and Products* 176: 114359. https://doi.org/10.1016/j.indcrop.2021.114359

Tao, J., Hosseinaei, O., Delbeck, L., Kim, P., Harper, D. P., Bozell, J. J., Rials, T. G. & Labbé, N. 2016. Effects of organosolv fractionation time on thermal and chemical properties of lignins. *RSC Advances* 6(82): 79228–79235. https://doi.org/10.1039/c6ra16296g

Wildschut, J., Smit, A. T., Reith, J. H. & Huijgen, W. J. J. 2013. Ethanol-based organosolv fractionation of wheat straw for the production of lignin and enzymatically digestible cellulose. *Bioresource Technology* 135: 58–66. https://doi.org/10.1016/j.biortech.2012.10.050

Wunna, K., Nakasaki, K., Auresenia, J., Abella, L. & Gaspillo, P. A. 2021. Enhancement of delignification and glucan content of sugarcane bagasse by alkali

pretreatment for bioethanol production. *ASEAN Journal of Chemical Engineering* 21(2): 133–142. https://doi.org/10.22146/ajche.59093

Wunna, K., Nakasaki, K., Auresenia, J. L., Abella, L. C. & Gaspillo, P. A. D. 2017. Effect of alkali pretreatment on removal of lignin from sugarcane bagasse. *Chemical Engineering Transactions* 56: 1831–1836. https://doi.org/10.3303/CET1756306

Yadav, P., Athanassiadis, D., Antonopoulou, I., Rova, U., Christakopoulos, P., Tysklind, M. & Matsakas, L. 2021. Environmental impact and cost assessment of a novel lignin production method. *Journal of Cleaner Production* 279: 123515. https://doi.org/10.1016/j.jclepro.2020.123515

Yousuf, A., Pirozzi, D. & Sannino, F. 2020. *Lignocellulosic Biomass to Liquid Biofuels*. Elsevier.

Zhang, Y., Wu, J. Q., Li, H., Yuan, T. Q., Wang, Y. Y. & Sun, R. C. 2017. Heat treatment of industrial alkaline lignin and its potential application as an adhesive for green wood-lignin composites. *ACS Sustainable Chemistry & Engineering* 5(8): 7269–7277. https://doi.org/10.1021/acssuschemeng.7b01485

Zhang, Z., Terrasson, V. & Guénin, E. 2021. Lignin nanoparticles and their nanocomposites. *Nanomaterials* 11(5): 1336. https://doi.org/10.3390/nano11051336